An analytic study of the switching process in excitonic optical bistability in semiconductors

1993 J. Phys.: Condens. Matter 5 4451

(http://iopscience.iop.org/0953-8984/5/26/016)

J. Phys.: Condens. Matter 5 (1993) 4451–4466. Printed in the UK

An analytic study of the switching process in excitonic optical bistability in semiconductors

Nguyen Ba An† and Paul Mandel

Optique Nonlinéaire Théorique, Université Libre de Bruxelles, Campus Plaine CP 231, B-1050 Bruxelles, Belgium

Received 22 January 1993, in final form 8 March 1993

Abstract. We study analytically the switching process in excitonic optical bistability in a semiconductor near the hysteresis limit points in the case of fully developed hysteresis. We consider four different time-dependent input pulse shapes that induce switching: a single rectangular pulse, a single triangular pulse, a sequence of rectangular pulses and a sequence of triangular pulses. The dependence of the switching time on the characteristics of these inputs is analysed.

1. Introduction

Since the observation of optical bistability (OB) in GaAs [1] and InSb [2], semiconductors have proved to be very good candidates for optically bistable devices. The most pronounced non-linearity in semiconductors is related to excitons whose binding energy is greatly enhanced by quantum confinement. Semiconductor quantum wells, quantum wires and quantum dots are thus of special interest with respect to practical devices. Furthermore, in excited semiconductors the photoabsorption may increase with increasing excitation density, leading to the appearance of the so-called intrinsic OB (see e.g. [3–6]) without any external feedback. Such an induced absorption mechanism makes experiment easier because the system can provide its own intrinsic feedback and one needs no special geometrical cavity configuration. This mechanism for intrinsic OB can thus be referred to as cavityless OB.

When a bistable device is operated as a memory element, an important factor is the switching time, i.e. the time required for the field to jump between its two stable steady states. This switching time controls the duty cycle, which is one of the figures of merit of a bistable device. In general, switching times are different for different non-linear devices and depend on specific characteristics of the systems. To obtain absolute values of switching times, one has to carry out elaborate numerical calculations, which, however, do not yield qualitative properties about other devices. Analytic results are therefore desirable to get generic information on a wide class of devices. However, this can be done only in some asymptotic limits. For example, the authors of [7] were able to give analytic expressions for the switching times in absorptive OB in the limit of large bistability parameter C (this parameter is defined in [8]). Their results showed the dependence of the up-switching (down-switching) process on the atomic (cavity) relaxation time. However, an alternative study of switching was performed using a local analysis valid near the limit points [9],

† On leave of absence from Institute of Theoretical Physics, PO Box 429 Boho, Hanoi 10000, Vietnam.

0953-8984/93/264451+16$07.50

in which the universal behaviour of a bistable device such as critical and/or non-critical slowing down could be theoretically predicted.

In this paper we extend the approach of [9] to switching in a semiconductor whose bistability is due to exciton–exciton interactions. In this connection we note that in [9] it was possible to derive a single characteristic equation depending on a unique parameter in the vicinity of the limit points. In the semiconductor excitonic OB there are more material parameters besides the input control [10]. Furthermore, two characteristic equations must be dealt with: one that describes the dependence of exciton density versus input pumping field, and the other that describes the dependence of photon density versus input pumping field [11, 12]. These features make the problem more complicated. Nevertheless, as will be shown in detail, an analytic treatment of the switching process is still possible. This can be achieved in two steps. First, we apply a scaling to reduce the number of relevant parameters to two. Secondly, we use the local expansion procedure proposed in [9] after performing a coordinate translation, which is necessary to separate adequately the two stable output branches of the OB curve.

We organize our paper as follows. In section 2, we model the semiconductor as an interacting exciton–photon system driven by an external coherent radiation field. Section 3 deals with the steady-state bistability. Section 4 is divided into five subsections. In the first subsection we analyse the stability of the steady solution, whereas the subsequent subsections are devoted to the study of the system response to a single rectangular (triangular) pulse as well as to a sequence of rectangular (triangular) pulses. The last section is a conclusion.

It should be stressed that our aim in this paper is not to obtain results valid for one specific semiconductor but rather to derive generic properties of the switching time and the switching mechanism that are independent of the precise nature of the underlying material considered. Thus the only explicit reference to semiconductor physics will be in section 2, where we derive the macroscopic equations from a *bona fide* microscopic Hamiltonian. The remaining sections are devoted to the analysis of the asymptotic time-dependent equations that describe the response of the medium to external pulses of different shapes. The material-independent solutions of these equations depend explicitly on the pulse characteristics. The motivation for considering switching by single and repeated pulses is linked to the fact that the ultrashort-pulse technique is now progressing quite fast. Our analytic treatment is expected to provide a guide for the use of controlling pulses in devices.

2. From the microscopic description to macroscopic equations

Generally, excited semiconductors contain various types of quasiparticles (charge carriers, excitons, biexcitons, optical/acoustic phonons, magnons, etc.) that interact with each other and with photons. This forms a genuine many-body quantum system. The electronic and optical properties of semiconductors must therefore be investigated at a microscopic level by taking into account the effects of damping and relaxation as well as the action of external fields [13]. However, even with such a powerful theoretical tool as the technique of non-equilibrium Green functions, it is not possible to solve the general semiconductor problem. Since we are concerned with excitonic OB, it is convenient to model the semiconductor as a quantum exciton–photon system. Even so, the model still faces the complexity connected with the non-bosonity of excitons, which are composite quasiparticles. Non-boson approaches to the many-exciton system have in fact been developed [14, 15], but their application seems difficult owing to the trilinear commutation relations and the normalization properties. Hence we shall work in the boson formalism [16] in which excitons are regarded as ideal bosons.

Let the semiconductor be pumped by an external coherent pump field with wavevector k, frequency Ω_k and amplitude $\mathcal{E}_k$. Inside the semiconductor the light is described in the second quantization representation by the photon annihilation (creation) operator b_k (b_k^+). The photon–exciton matrix element and the exciton–exciton interaction are respectively denoted by g and f, which are assumed for simplicity to be k-independent. Considering only the coherent exciton, the model Hamiltonian can be formulated in the form [17]

$$H = E_k a_k^+ a_k + \Omega_k b_k^+ b_k - g(a_k^+ b_k + b_k^+ a_k) + (1/V) f a_k^+ a_k^+ a_k a_k + \mathrm{i}(\Omega_k V)^{1/2} \times [\mathcal{E}_k \exp(-\mathrm{i}\Omega_k \tau) b_k^+ - \mathcal{E}_k^* \exp(\mathrm{i}\Omega_k \tau) b_k] \tag{2.1}$$

where the unit system used is $\hbar = c = 1$, V is the sample volume, and a_k (a_k^+) is the annihilation (creation) operator of the coherent exciton with momentum k and energy E_k. This model Hamiltonian can be derived from the original electron–hole Coulomb Hamiltonian [16]. The f coupling constant comprises several terms, which describe direct as well as exchange Coulomb interactions between the constituents of two excitons. The explicit dependence of f on momentum and spin has been obtained in [18]. The Heisenberg equations for the k mode of the exciton and the photon can be set up from (2.1):

$$\mathrm{d}a_k/\mathrm{d}\tau = -\mathrm{i}(E_k - \mathrm{i}\gamma_\mathrm{a}) a_k + \mathrm{i}g b_k - (2\mathrm{i}f/V) a_k^+ a_k a_k \tag{2.2}$$

$$\mathrm{d}b_k/\mathrm{d}\tau = -\mathrm{i}(\Omega_k - \mathrm{i}\gamma_\mathrm{b}) b_k + \mathrm{i}g a_k + (\Omega_k V)^{1/2} \mathcal{E}_k \exp(-\mathrm{i}\Omega_k \tau) \tag{2.3}$$

where γ_a (γ_b) is the exciton (photon) transverse damping, which has been added phenomenologically. To study the macroscopic transient evolution we need to average (2.2) and (2.3) over the coherent state [19] of the field to get the averages $\langle a_k(\tau)\rangle$ and $\langle b_k(\tau)\rangle$. Because the coherent state is the eigenstate of the annihilation operator, we can use the following factorization:

$$\langle a_k^+ a_k a_k\rangle = n_k \langle a_k\rangle \tag{2.4}$$

where $n_k \equiv |\langle a_k\rangle|^2$. With the aid of (2.4), we obtain from (2.2) and (2.3) a closed pair of equations for $\langle a_k(\tau)\rangle$ and $\langle b_k(\tau)\rangle$, i.e.

$$\mathrm{d}\langle a(\tau)\rangle/\mathrm{d}\tau = -\mathrm{i}(E + 2f\rho - \mathrm{i}\gamma_\mathrm{a})\langle a(\tau)\rangle + \mathrm{i}g\langle b(\tau)\rangle \tag{2.5}$$

$$\mathrm{d}\langle b(\tau)\rangle/\mathrm{d}\tau = -\mathrm{i}(\Omega - \mathrm{i}\gamma_\mathrm{b})\langle b(\tau)\rangle + \mathrm{i}g\langle a(\tau)\rangle + (\Omega V)^{1/2}\mathcal{E}\mathrm{e}^{-\mathrm{i}\Omega\tau}. \tag{2.6}$$

In (2.5) and (2.6) and in the remainder of this paper we shall everywhere drop the index k for convenience. The parameter ρ is the density of the coherent exciton, $\rho = V^{-1}|\langle a(\tau)\rangle|^2$. Since the time dependence of the system is mostly imposed by the driving field, we can extract from $\langle a(\tau)\rangle$ and $\langle b(\tau)\rangle$ the slowly varying functions $\xi_{\mathrm{a,b}}(\tau)$ and $\zeta_{\mathrm{a,b}}(\tau)$:

$$\langle a(\tau)\rangle = Q_\mathrm{a}[\xi_\mathrm{a}(\tau) + \mathrm{i}\zeta_\mathrm{a}(\tau)]\mathrm{e}^{-\mathrm{i}\Omega\tau} \tag{2.7}$$

$$\langle b(\tau)\rangle = Q_\mathrm{b}[\xi_\mathrm{b}(\tau) + \mathrm{i}\zeta_\mathrm{b}(\tau)]\mathrm{e}^{-\mathrm{i}\Omega\tau} \tag{2.8}$$

with the coefficients $Q_\mathrm{a} = [\gamma_\mathrm{a} V/(2f)]^{1/2}$ and $Q_\mathrm{b} = Q_\mathrm{a}\gamma_\mathrm{b}/g$. Setting the reference phase such that $\mathcal{E}$ is real, we can substitute (2.7), (2.8) into (2.5), (2.6) and introduce the scalings

$$\tilde{\tau} = \tau\gamma_\mathrm{a} \qquad G = (\Omega - E)/\gamma_\mathrm{a} \qquad M = \gamma_\mathrm{b}/\gamma_\mathrm{a}$$
$$D = (g/\gamma_\mathrm{a})^2 \qquad P = g\mathcal{E}(2\Omega f/\gamma_\mathrm{a}^5)^{1/2} \tag{2.9}$$

to arrive at the following macroscopic set of non-linear differential equations for $\xi_{a,b}$ and $\zeta_{a,b}$:

$$d\xi_a/d\tilde{\tau} = -\xi_a - (G - \xi_a^2 - \zeta_a^2)\zeta_a - \zeta_b \tag{2.10}$$

$$d\zeta_a/d\tilde{\tau} = -\zeta_a + (G - \xi_a^2 - \zeta_a^2)\xi_a + \xi_b \tag{2.11}$$

$$d\xi_b/d\tilde{\tau} = -M\xi_b - D\zeta_a + P \tag{2.12}$$

$$d\zeta_b/d\tilde{\tau} = -M\zeta_b + D\xi_a. \tag{2.13}$$

In principle, the set (2.10) to (2.13) fully describes the dynamics of the system, including both regular and chaotic self-pulsations. Here, our aim is to investigate the switching dynamics in the case in which the system develops a steady hysteresis. To this end, it suffices to study the scaled exciton and photon numbers defined as

$$N_a = \xi_a^2 + \zeta_a^2 \qquad N_b = \xi_b^2 + \zeta_b^2. \tag{2.14}$$

Making use of (2.10)–(2.13) we can write the dynamical equations for N_a and N_b in the form

$$dN_a/d\tilde{\tau} = -N_a + I/[(N_a - G)^2 + B] \tag{2.15}$$

$$dN_b/d\tilde{\tau} = -N_b + I[(N_a - G)^2 + 1]/[(N_a - G)^2 + B] \tag{2.16}$$

with

$$I = (P/M)^2 \qquad \text{and} \qquad B = (1 + D/M)^2. \tag{2.17}$$

It is worth noticing that, apart from the input control parameter $I \sim P^2 \sim \mathcal{E}^2$, we have reduced the number of material parameters from six (E, Ω, f, g, γ_a, γ_b) in equations (2.2) and (2.3) to three (G, M, D) in (2.10)–(2.13) and then to two (G, B) in (2.15) and (2.16) by the appropriate scalings (2.7)–(2.9) and (2.17). A further reduction to only one parameter will be discussed in the next section.

3. Steady-state bistability

In the steady regime we get from (2.15) and (2.16)

$$I = N_a[(N_a - G)^2 + B] \tag{3.1}$$

$$N_b = N_a[(N_a - G)^2 + 1]. \tag{3.2}$$

For $G > (3B)^{1/2}$ the curve $N_a = N_a(I)$ given by (3.1) will be S-shaped as schematically illustrated in figure 1(a). This is the light-excitation density bistability. Since $B > 1$ by the definition (2.17), the condition $G > (3B)^{1/2}$ automatically yields $G > \sqrt{3}$, which means that the curve of $N_a = N_a(N_b)$ given by (3.2) is also S-shaped. Because the output field is proportional to N_b, the curve $N_b = N_b(I)$ can be referred to as the output–input characteristic of the optical system and thus we shall be interested in the dependence of N_b on I rather than of N_a on I. As has been shown in [20] and in more detail in [21],

the corresponding shapes of the curve $N_b = N_b(I)$ may have very distinct topologies. For $G \gg (3B)^{1/2}$, i.e. for large exciton detuning and small exciton transverse damping, the system will display a fully developed bistability with very large hysteresis. In such an asymptotic situation, it is useful to define a small parameter $\epsilon = 1/G$. We then have $R = (3B/2)^{1/2} = O(1)$. In the next section we shall see that the parameter R can be absorbed in a new scaling so that ϵ will remain the only parameter of the problem. The key assumption of fully developed bistability leaves us with a parameter ϵ in terms of which all others will be expanded. For instance, the intensity of the limit points labelled 2 and 3 on figure 1(*a*) are $I_2 = 4/(3\epsilon)^3 + O(\epsilon^{-1})$ and $I_3 = 2R^2/(3\epsilon) + O(\epsilon)$. When $I = I_2$, the value of N_a at the limit point is $N_{a2} = 1/(3\epsilon) + R^2\epsilon/3 + O(\epsilon^3)$, while the corresponding value of N_a on the upper branch is $N_{a4} = 4/(3\epsilon) + O(\epsilon)$. Similarly, when $I = I_3$, we have $N_{a3} = 1/\epsilon - R^2\epsilon/3 + O(\epsilon^3)$ and $N_{a1} = 2R^2\epsilon/3 + O(\epsilon^3)$. A similar analysis can be performed to estimate the leading contribution to N_b at the four special points of the curve $N_b = N_b(I)$. For $I = I_2$, we have $N_{b2} = 4/(3\epsilon)^3 - (2R^2/3 - 1)/(3\epsilon) + O(\epsilon)$ and $N_{b4} = 4/(3\epsilon)^3 - 4(2R^2/3 - 1)/(3\epsilon) + O(\epsilon)$. For the other limit point, at I_3, we have $N_{b3} = 1/\epsilon + O(\epsilon)$ and $N_{b1} = 2R^2/(3\epsilon) + O(\epsilon)$.

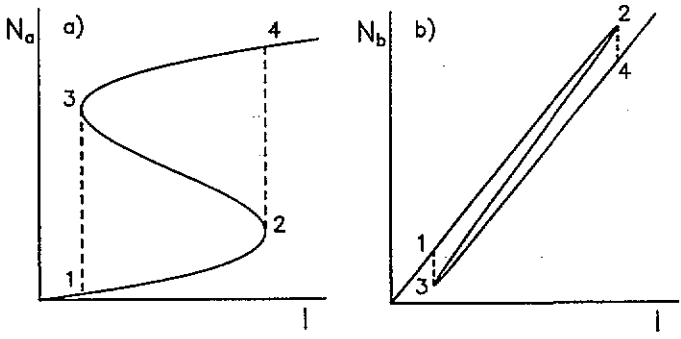

Figure 1. Schematic dependence of (*a*) the scaled exciton number N_a and (*b*) the scaled photon number N_b versus the scaled input intensity I in the limit of fully developed bistability.

4. Analytic local treatment around the limit points

As demonstrated in [9], a local analysis works well when the vicinity of a limit point (point 2 or point 3 in figure 1) is far from the third steady branch corresponding to the same input intensity (point 4 or point 1 in figure 1). Taking into account the asymptotic expansion determined in the previous section, we see that the coordinates of point 1 and point 3 in figure 1(*b*) have the same dominant order of magnitude in ϵ. This is also true for point 2 and point 4. This fact prevents the direct scaling procedure made in [9]. However, if we first translate the origin of the coordinate system to the limit point 3 in figure 1(*b*), then the distance from point 1 to the new origin is given by $(B - 1)/\epsilon$, which is a very large positive value. The same large distance from the origin holds for points 2 and 4. Thus, by the translation of the coordinate system we can again consider the third steady branch as located at a large distance of order $O(\epsilon^{-1})$ from the limit point. For definiteness we shall present a detailed local analysis only around point 3. A similar treatment can also be done in the vicinity of point 2.

Translating the origin of the coordinate system to point 3 and considering only the vicinity of this point means that we introduce the new O(1) variables y, z and p through:

$$N_a = N_{a3} + \epsilon y + O(\epsilon^2) \tag{4.1}$$

$$N_b = N_{b3} - \epsilon z + O(\epsilon^2) \tag{4.2}$$

$$I = I_3 + \epsilon p + O(\epsilon^2) \tag{4.3}$$

with N_{a3}, N_{b3} and I_3 being the solutions of the steady-state equations (3.1) and (3.2). Inserting (4.1), (4.2) and (4.3) into (2.15), (2.16) and using the expansions of N_{a3}, N_{b3} and I_3 obtained in the previous section, we have derived to dominant order in ϵ the following dynamical equations for the new variables:

$$dy/dt = p - y^2 \tag{4.4}$$

$$dz/dt = -p + y^2 - B(y + z) \tag{4.5}$$

where $t = \tilde{\tau}/B$. Equations (4.4) and (4.5) can be combined to give:

$$d(y + z)/d\tilde{\tau} = -(y + z) \tag{4.6}$$

which yields

$$z(\tilde{\tau}) = -y(\tilde{\tau}) + [y(0) + z(0)]e^{-\tilde{\tau}}. \tag{4.7}$$

No essential feature of the problem will be lost if we choose $y(0) + z(0) = 0$. Then the sum $y + z$ is an invariant of the motion, which will simplify the analytic study of (4.4) and (4.5).

4.1. Stability of the steady solution

From (4.4) and (4.5) it follows that the steady solutions are of the form

$$z_\pm = \pm p^{1/2}. \tag{4.8}$$

The vicinity of point 3 in figure 1(*b*) is replaced by a parabola emerging from the origin in the (p, z) plane. We shall call z_+ (z_-) the upper (lower) branch of the asymptotic parabola, which in fact corresponds to the middle (lower) branch 3–2 (3–4) of the global bistability curve represented in figure 1(*b*). For a constant input p the time-dependent solution of (4.4) and (4.5) is

$$z(t) = \frac{z(0) - z_+ \tanh(z_+ t)}{z_+ - z(0)\tanh(z_+ t)} z_+. \tag{4.9}$$

If the system is initially near the upper steady branch z_+, i.e. $z(0) = z_+ + \alpha$ with $|\alpha| \ll 1$, equation (4.9) becomes

$$z(t) = \frac{z_+ + \alpha - z_+ \tanh(z_+ t)}{z_+ - (z_+ + \alpha)\tanh(z_+ t)} z_+. \tag{4.10}$$

If $\alpha = 0$, equation (4.10) gives

$$z(t) \equiv z_+. \tag{4.11}$$

If $\alpha < 0$ the denominator of (4.10) remains always positive but its numerator may vanish at $t = t_1$ with

$$t_1 = (1/z_+)\tanh^{-1}[(z_+ + \alpha)/z_+]. \tag{4.12}$$

For $t > t_1$, the function $\tanh(t)$ tends to unity and $z(t)$ tends to $-z_+ = z_-$. That means that the system being initially near but below ($\alpha < 0$) to the upper branch (z_+) relaxes to the lower branch (z_-). The relaxation time depends on α. Larger $|\alpha|$ will result in faster relaxation. However, if $\alpha > 0$ the numerator of (4.10) is always positive but its denominator vanishes at $t = t_2$ with

$$t_2 = (1/z_+) \tanh^{-1}[z_+/(z_+ + \alpha)]. \tag{4.13}$$

When t varies from zero to t_2, the denominator of (4.10) varies from z_+ to 0 and hence $z(t)$ tends to $+\infty$. Since in our local model the third steady branch of the global curve (branch 1–2 in figure 1(*b*)) lies at infinity, the divergence of $z(t)$ means the jump to the third branch when $\alpha > 0$. Equation (4.13) shows that the jump time t_2 will be shorter for larger α. The solution of (4.4) and (4.5) after t_2 is physically irrelevant within the local model. These results imply that the upper branch z_+ is unstable and the lower branch z_- is stable. This will also be true for the corresponding branches of the global curves, i.e. the middle branch 3–2 is unstable and the lower branch 3–4 is stable, at least near the limit point.

4.2. Switching by a rectangular pulse

We consider now the response of our system to several kinds of input control fields that vary in time and determine their influence on the switching properties of the device. In this subsection we consider the input control in the form of a single rectangular pulse. Suppose that $t = 0$ the system is kept near the limit point 3 on the stable lower branch corresponding to a holding intensity $p_0 > 0$, i.e. $z_0 \equiv z(0) = -p_0^{1/2}$. A rectangular pulse of amplitude A and duration T is added to the holding intensity p_0 as schematically illustrated in figure 2(*a*). This physical problem is mathematically formulated as the solution of (4.4) and (4.5) with the time-dependent $p = p(t)$,

$$p(t) = \begin{cases} p_0 & \text{for } t \leqslant 0 \\ p_0 - A & \text{for } 0 \leqslant t \leqslant T \\ p_0 & \text{for } T \leqslant t \end{cases} \tag{4.14}$$

and with the initial condition

$$z_0 \equiv z(0) = -p_0^{1/2}. \tag{4.15}$$

The solution is

$$z(t) = \begin{cases} z_1(t) & \text{for } 0 \leqslant t \leqslant T \\ z_2(t) & \text{for } T \leqslant t \end{cases} \tag{4.16}$$

where

$$z_1(t) = \frac{(A - p_0)^{1/2} \tan[t(A - p_0)^{1/2}] - p_0^{1/2}}{1 + [p_0/(A - p_0)]^{1/2} \tan[t(A - p_0)^{1/2}]} \tag{4.17}$$

$$z_2(t) = \frac{z_1(T) - p_0^{1/2} \tanh[(t - T)p_0^{1/2}]}{1 - (1/p_0)^{1/2} z_1(T) \tanh[(t - T)p_0^{1/2}]}. \tag{4.18}$$

For a given pulse amplitude $A > p_0$, it is easy to verify that $z_1(t)$ increases with increasing t while z_2 as a function of $t - T$ increases (decreases) with increasing $t - T$ if $z_1(T) > p_0^{1/2}$

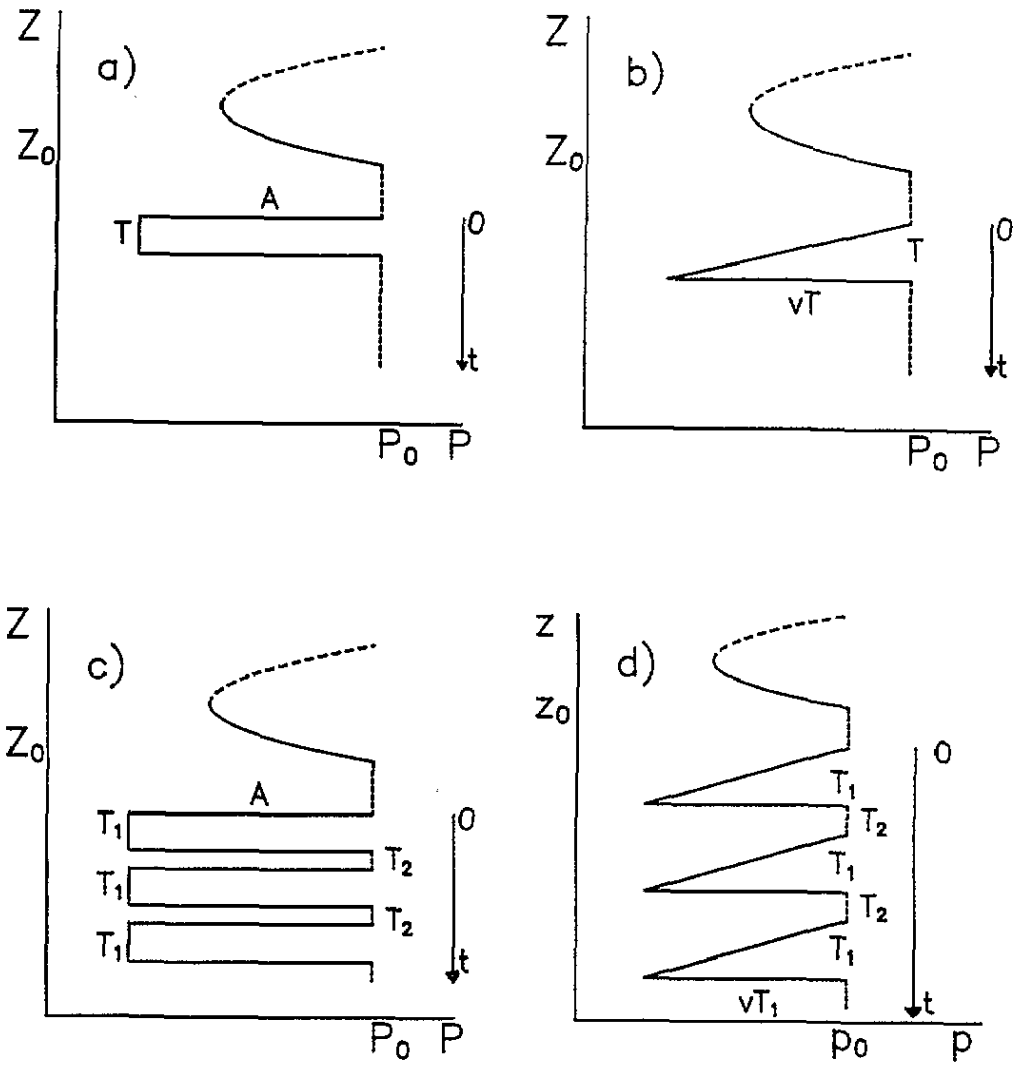

Figure 2. Local two-branch system under the action of (*a*) a single rectangular pulse, (*b*) a single triangular pulse, (*c*) a sequence of rectangular pulses and (*d*) a sequence of triangular pulses. The upper long-dashed (lower solid) branch represents the unstable (stable) steady state z_+ (z_-). Vertical short-dashed lines show the holding intensity p_0 corresponding to the initial state z_0.

(if $z_1(T) < p_0^{1/2}$). Therefore, there must exist a critical pulse duration that separates the two time regions with very different dynamical behaviour. Denoting this critical duration by T_c it is determined by the implicit equation

$$z_1(T_c) = p_0^{1/2}. \tag{4.19}$$

Physically, the system behaviour is understood as follows. When $T < T_c$ the system first follows the solution z_1 until the pulse is over. After that it must return via z_2 to its initial state (see figure 3(*a*), curves with numbers 3 and 6). No jump occurs in this case. When $T = T_c$ the system has enough time to arrive at the other steady solution $z = p_0^{1/2}$

but then stays there because it is a solution of the problem (figure 3(*a*), curve with number 8.5446). When $T > T_c$ the system is able to cross the upper branch before the pulse ends. Hence, after the end of the pulse, the system follows z_2 to infinity because now z_2 is an increasing function of time (figure 3(*a*), curve with number 9). This models the dynamics of a jump. When T is much greater than T_c the jump may take place in a very short time because in this case the system can switch up during part of the pulse action (figure 3(*a*), curve with number 11). Let us try to get some insight into the nature of slowing down near T_c. From (4.19) and (4.17), T_c is explicitly given by

$$T_c = \frac{1}{(A-p_0)^{1/2}} \tan^{-1}\left(\frac{2[p_0(A-p_0)]^{1/2}}{A-2p_0}\right). \tag{4.20}$$

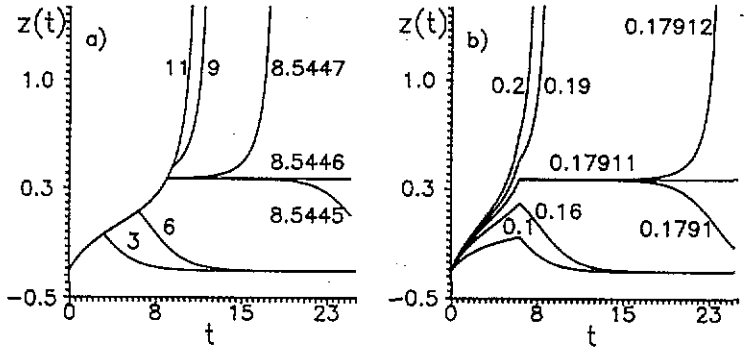

Figure 3. Time evolution under a single rectangular pulse and the holding intensity $p_0 = 0.1$. (*a*) $A = 0.15$, $T_c = 8.5446$. Values of T are indicated near each curve. Non-critical slowing down is shown by the curves with $T = 8.5447$, 8.5446 and 8.5445. (*b*) $T = 6$, $A_c = 0.179\,11$. Values of A are indicated near each curve. Non-critical slowing down is shown by the curves with $A = 0.179\,12$, $0.179\,11$ and $0.179\,10$.

As to the switching time, T_s, it is the time needed for the system to diverge. The explicit expression for T_s is ($T > T_c$)

$$T_s = T + \frac{1}{(A-p_0)^{1/2}} \tan^{-1}\left[\left(\frac{p_0}{A-p_0}\right)^{1/2}\right] + \frac{1}{2p_0^{1/2}} \ln\left(\frac{z_1(T)+p_0^{1/2}}{z_1(T)-p_0^{1/2}}\right). \tag{4.21}$$

For $T < T_c$ it is natural to introduce the relaxation time, i.e. the time it takes for the system after failing to make a jump to come back to its initial state. For simplicity, we define a relaxation time only when $z(T) > 0$. The relaxation time, T_R, can then be defined when $T < T_c$ as the time needed to decay from $z(T)$ down to $z(t) = 0$:

$$T_R = \frac{1}{2p_0^{1/2}} \ln\left(\frac{z_1(T)-p_0^{1/2}}{z_1(T)+p_0^{1/2}}\right). \tag{4.22}$$

From (4.20) and (4.21) we see that both T_c and T_s diverge as $1/(A-p_0)^{1/2}$ when $A \to p_0$. This divergence is a manifestation of critical slowing down, which is a universal phenomenon always occurring in the vicinity of a critical point [9, 22]. However, there may

arise another type of slowing down that is not associated with the vicinity of the critical points. In fact, even for $A - p_0 = O(1)$ but $T = T_c \pm \lambda^2$ ($\lambda \ll 1$) the switching and the relaxation times diverge logarithmically. When $T = T_c + \lambda^2$ the logarithmic divergence appears in T_s (figure 3(a), curve with number 8.5447):

$$T_s \simeq \ln(2p_0^{1/2}/\beta) \tag{4.23}$$

where

$$\beta = A\lambda^2/\{1 + [p_0/(A - p_0)]^{1/2} \tan[T_c(A - p_0)^{1/2}]\} \ll 1 \tag{4.24}$$

and when $T = T_c - \lambda^2$ this divergence affects T_R (figure 3(a), curve with number 8.5445):

$$T_R \simeq \ln(2p_0^{1/2}/\beta) \tag{4.25}$$

with β given by (4.24). The slowing down governed by (4.23) and (4.25) is called non-critical slowing down and the first quantitative experimental observation was reported in [23].

An alternative way to control the dynamical switching is to keep the pulse duration fixed and alter its amplitude. It can be proved that for a given T there exists a critical amplitude A_c, which is determined by the implicit equation

$$A_c = p_0 + \frac{1}{T^2}\left[\tan^{-1}\left(\frac{2[p_0(A_c - p_0)]^{1/2}}{A_c - 2p_0}\right)\right]^2 \tag{4.26}$$

such that when $A > A_c$ ($A < A_c$) the switching is possible (impossible). In figure 3(b) we display the time evolution of the system when $T = 6$. The corresponding pulse critical amplitude is given by $A_c = 0.179\,11$. It is clearly seen that only pulses with $A > A_c$ are able to switch up the system. Non-critical slowing down also occurs when A is near A_c (see figure 3(b), curves with $A = 0.179\,12$, $0.179\,11$ and $0.179\,10$). Quite interestingly, our figure 3(b) resembles very much the experimental data of a Schmitt trigger circuit and of the sodium experiments reported in [24]. Although our paper deals with semiconductors, this resemblance is reasonable since after making an adequate scaling of the physical parameters, we are left with a generic problem, which is the dynamics in the vicinity of a limit point. The difference, however, is that here we have to deal with a pair of equations, while in the previously reported cases a single equation was sufficient to characterize the local dynamics in the vicinity of the limit point.

Summing up the results obtained so far we see that, for the realization of a switching process, a smaller pulse amplitude requires a longer pulse duration and, vice versa, a shorter pulse duration needs a larger pulse amplitude. Such remarks express the role of the pulse area. However, the analytic dependence on the pulse area can be derived only in a particular case when the system is initially very near the limit point [25]. The relations between the critical pulse duration T_c (amplitude A_c) and its amplitude A (duration T) are drawn in figure 4 as a function of p_0. The figures show that for a given amplitude A (duration T) the corresponding critical duration T_c (amplitude A_c) should be shorter (smaller) if the system is nearer to the limit point, i.e. if p_0 is smaller. In the limit of vanishing p_0, i.e. $p_0 = \delta^2 \ll 1$, equation (4.26) yields, to dominant order in δ, $(AT)_c \equiv A_cT = 2\delta$. In other words, in this limit all that matters is the product of A and T, i.e. the pulse area, rather than the characteristics of each pulse separately.

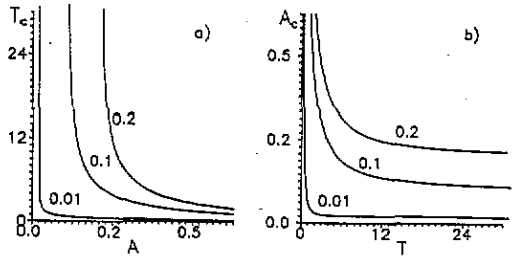

Figure 4. (*a*) Critical pulse duration T_c versus pulse amplitude A for various values of the holding intensity p_0 (indicated near each curve). (*b*) Similar dependence but of critical pulse amplitude A_c versus its duration T.

4.3. Switching by a triangular pulse

This subsection deals with the switching under the action of a single triangular pulse (see figure 2(*b*)). The motivation to consider such a kind of pulse is that experiments are traditionally carried out by sweeping the control parameter slowly across the critical region to allow the system to follow adiabatically the steady state. The two characteristics of this pulse are the sweep rate v and the duration T of the sweep. As shown in [9], such a problem can be solved analytically in terms of the Airy functions. The solution of (4.4) and (4.5) with the initial condition (4.15) and the sweep control parameter $p = p(t)$

$$p(t) = \begin{cases} p_0 & \text{for } t \leqslant 0 \\ p_0 - vt & \text{for } 0 \leqslant t \leqslant T \\ p_0 & \text{for } T \leqslant t \end{cases} \tag{4.27}$$

can again be written in the form (4.16) but with $z_1(t)$ being defined by

$$z_1(t) = v^{1/3}\frac{\mathrm{Ai}'(\chi) + \eta\mathrm{Bi}'(\chi)}{\mathrm{Ai}(\chi) + \eta\mathrm{Bi}(\chi)} \tag{4.28}$$

where

$$\chi = (p_0 - vt)v^{-2/3} \tag{4.29}$$

and η is determined by the initial condition,

$$\eta = -\frac{v^{1/3}\mathrm{Ai}'(p_0v^{-2/3}) + p_0^{1/2}\mathrm{Ai}(p_0v^{-2/3})}{v^{1/3}\mathrm{Bi}'(p_0v^{-2/3}) + p_0^{1/2}\mathrm{Bi}(p_0v^{-2/3})}. \tag{4.30}$$

In (4.28) and (4.30) Ai, Bi and Ai′, Bi′ are the Airy functions and their derivatives [26]. To control the dynamics of switching, one may either fix the sweep duration and change the sweep rate or keep the sweep rate unchanged but adjust the duration of sweep. For a fixed sweep duration T, the sweep rate must be large enough to cause a switching. Thus there will exist a critical sweep rate, v_c, dependent on both T and p_0, which separates the domain of switching from the domain of decay back to the lower state. Since $z_2(t)$ is the same as in the case of a rectangular pulse, we can immediately determine v_c by the implicit formula

$$v_c = p_0^{2/3}\left(\frac{\mathrm{Ai}(\chi_c) + \eta_c\mathrm{Bi}(\chi_c)}{\mathrm{Ai}'(\chi_c) + \eta_c\mathrm{Bi}'(\chi_c)}\right)^3 \tag{4.31}$$

with

$$\chi_c = (p_0 - v_c T)v_c^{-2/3}$$
$$\eta_c = -\frac{v_c^{1/3}\mathrm{Ai}'(p_0 v_c^{-2/3}) + p_0^{1/2}\mathrm{Ai}(p_0 v_c^{-2/3})}{v_c^{1/3}\mathrm{Bi}'(p_0 v_c^{-2/3}) + p_0^{1/2}\mathrm{Bi}(p_0 v_c^{-2/3})}. \tag{4.32}$$

The time evolution is now represented by a parametric plot in the zp plane (figure 5(a)) because we want to compare the static and the dynamic solutions. As seen from figure 5(a), the slower the sweep rate the closer the time-dependent trajectory remains near the steady stable state curve, which is the (lower) long-dashed curve. In the limit of $v \ll 1$ and when $vt < p_0$ the argument of the Airy functions becomes very large and positive. Then these special functions have a dominant exponential decay and to dominant order in v we have

$$z_1(t) = -v^{1/3}\chi^{1/2} \equiv -(p_0 - vt)^{1/2} = -[p(t)]^{1/2}. \tag{4.33}$$

Comparing this result with (4.8), it confirms that for a very slow sweep the system indeed follows adiabatically the lower steady stable state but only as long as it remains far from the limit point. In general, (4.28) is valid for arbitrary v, T, p_0 and t, and the system follows its own time-dependent trajectory as shown in figure 5(a). For increasing time z grows in the direction indicated by the arrows. Curve 3 in the figure corresponds to $v = v_c = 0.008\,873$ for $T = 20$. At $t = T$, the sweep stops exactly on the upper steady state $p_0^{1/2}$ where it remains in the absence of perturbations that would destabilize it. For $v < v_c$ there is relaxation back to the initial state (curves 1 and 2). For $v > v_c$ the switching takes place in a finite time $T_s > T$ after the sweep is finished (curves 4 and 5) or even in a time shorter than T, if the sweep rate is very high (curve 6). In figure 5(b) we trace the time-dependent trajectories when v is kept constant, $v = 0.01$ and T varies. The critical sweep duration is $T_c = 18.3205$.

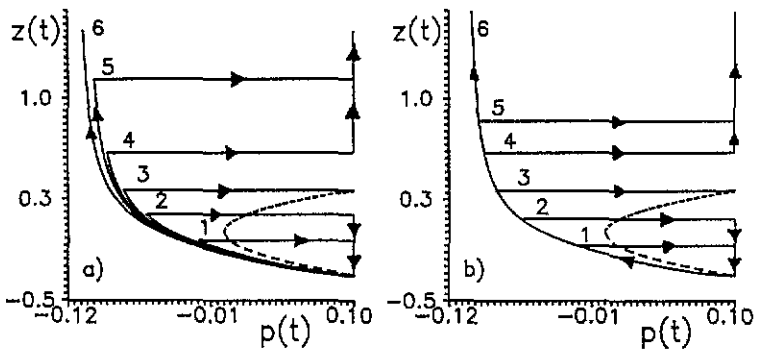

Figure 5. Time-dependent attractor in the (z, p) plane in the case of sweep by a single triangular pulse, for $p_0 = 0.1$. (a) $T = 20$. Curves 1, 2, 3, 4, 5 and 6 correspond to $v = 0.006$, 0.008, 0.008 873 ($= v_c$), 0.0095, 0.010 and 0.011, respectively. (b) $v = 0.01$. Curves 1, 2, 3, 4, 5 and 6 correspond to $T = 12$, 16.5, 18.3205 ($= T_c$), 19.3, 19.7 and 20, respectively. In both (a) and (b) the arrows indicate the time-evolution direction. The upper short-dashed (lower long-dashed) branch of the parabola is the steady unstable (stable) state.

4.4. Switching by a sequence of rectangular pulses

In practice, pulses with too large amplitude and too long duration cause a non-negligible heating of the device that may obscure or even quench the desirable optical effect. This is particularly important for those effects originating from excitons, because the binding energy of the latter is small and thus they could be destroyed by means of heat. The thermal gradient induced by the input power might also reduce the performance of the device. A possible alternative to control the system is to apply a sequence of pulses, each of which has relatively small amplitude and short duration. As will be shown in this and in the next subsection, a sequence of pulses may induce switching in somewhat longer time but with less sample heating. In this subsection, we deal with a sequence of rectangular pulses (figure 2(*c*)). Each pulse has an amplitude A and an 'action duration' T_1. They are separated in time by T_2 (the 'out-of-action duration'). We now have three parameters to control: A, T_1 and T_2. For $T_2 \gg T_1$ the pulse sequence will act like a single pulse with amplitude A and duration T_1. Of interest is the situation when T_2 is comparable with or less than T_1. It turns out that, even in this case, the problem can be solved exactly for arbitrary A, T_1 and T_2. The solution is written in the form:

$$z(t) = \begin{cases} z_1(t) & \text{for } 0 \leqslant t \leqslant T_1 \\ z_2(t) & \text{for } T_1 \leqslant t \leqslant T_1 + T_2 \\ z_3(t) & \text{for } T_1 + T_2 \leqslant t \leqslant 2T_1 + T_2 \\ \dots & \end{cases} \tag{4.34}$$

where $z_{2n-1}(t)$ is the solution in the time interval $(n-1)(T_1+T_2) \leqslant t \leqslant (n-1)(T_1+T_2)+T_1$, while the time interval for $z_{2n}(t)$ is $n(T_1+T_2)-T_2 \leqslant t \leqslant n(T_1+T_2)$. The analytic expressions for $z_{2n-1}(t)$ and $z_{2n}(t)$ are

$$\begin{aligned} z_{2n-1}(t) = {} & [\![z_{2n-2}[(n-1)(T_1+T_2)] + (A-p_0)^{1/2}\tan\{[t-(n-1)(T_1+T_2)](A-p_0)^{1/2}\}]\!] \\ & \times [\![1-[1/(A-p_0)]^{1/2} z_{2n-2}[(n-1)(T_1+T_2)] \\ & \times \tan\{[t-(n-1)(T_1+T_2)](A-p_0)^{1/2}\}]\!]^{-1} \end{aligned} \tag{4.35}$$

$$z_{2n}(t) = \frac{z_{2n-1}[nT_1+(n-1)T_2] + p_0^{1/2}\tanh\{[t-nT_1-(n-1)T_2]p_0^{1/2}\}}{1-(1/p_0)^{1/2} z_{2n-1}[nT_1+(n-1)T_2]\tanh\{[t-nT_1-(n-1)T_2]p_0^{1/2}\}} \tag{4.36}$$

with $z_0 \equiv z(0)$. In figure 6(*a*) we illustrate z as a function of t for $p_0 = 0.1$, $A = 0.15$, $T_1 = 4$ and $T_2 = 2$. We have on purpose chosen $T_1 = 4$, which is much less than the critical pulse duration $T_c = 8.5445$ corresponding to $A = 0.15$ in the case of a single pulse (see figure 3(*a*)). As seen from figure 6(*a*), a switching is eventually possible even for such a small value of T_1. This is in clear contrast with the action of a single pulse. In fact the system will require a longer time to make an actual jump. It first has to undergo a quite long zig-zag path before the actual switching occurs. The zig-zag time evolution of figure 6(*a*) looks very much like that observed by the experimental measurement in the Schmitt trigger circuit and also like that obtained by an approximated analytical solution of a switching process operated under a periodically modulated input control (see [27]). In order to emphasize the relative role of T_1 and T_2 we represent in figures 6(*b*) and (*c*) the evolution of $z(t)$ with different relations between T_1 and T_2. Figure 6(*b*) is a plot with the constant $T_2 = 1$ but $T_1 = 4$, 5 and 7. In figure 6(*c*) instead, $T_1 = 4$ and $T_2 = 1$, 1.5 and

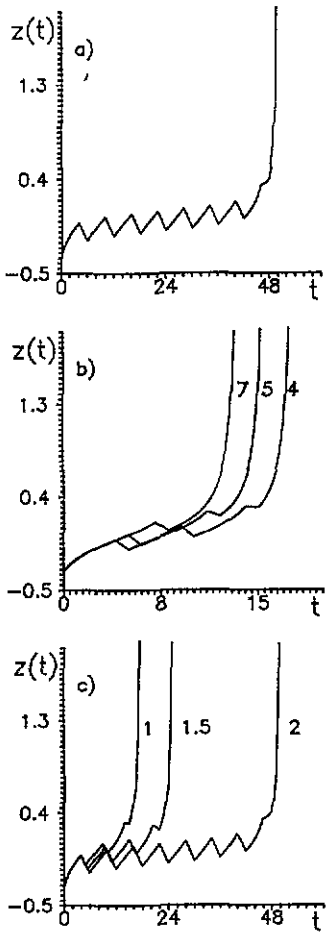

Figure 6. Switching by a sequence of rectangular pulses, for $p_0 = 0.1$, $A = 0.15$. (*a*) $T_1 = 4$, $T_2 = 2$. The switching eventually occurs after a long zig-zag evolution. (*b*) $T_2 = 1$, $T_1 = 4$, 5 and 7 (values of T_1 are indicated near each curve). (*c*) $T_1 = 4$, $T_2 = 1$, 1.5 and 2 (values of T_2 are near each curve).

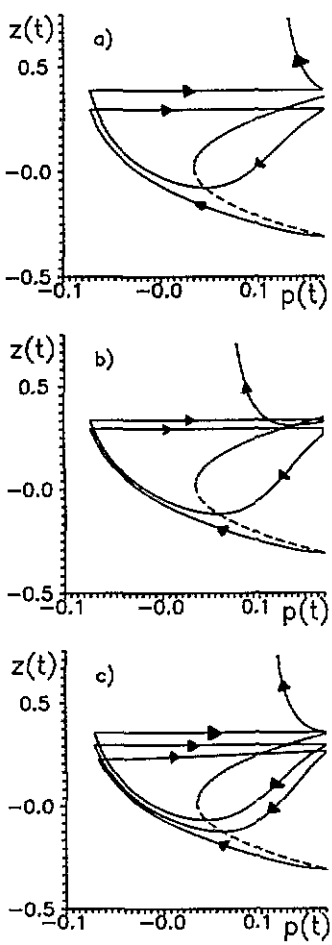

Figure 7. Switching by a sequence of triangular pulses presented as a parametric plot in the (z, p) plane, for $p_0 = 0.1$ and $v = 0.01$. (*a*) $T_1 = 18$, $T_2 = 0.2$, (*b*) $T_1 = 18$, $T_2 = 0.8$ and (*c*) $T_1 = 17.8$, $T_2 = 0.2$. In (*a*), (*b*) and (*c*) the arrows indicate the time-evolution direction. The steady states are also represented as in figure 5.

2. These figures indicate that the switching will be faster for longer T_1 and/or shorter T_2 as intuitively expected. Our results provide a basis to evaluate these effects qualitatively.

Let us again note that the idea of using periodic control inputs might be of interest in applications for at least two reasons. First, it requires relatively small amplitude and short action duration of each pulse. Secondly, it reduces effects connected with thermal gradients because the average power of a periodic input is constant. The latter aspect is especially relevant for integrated devices.

4.5. Switching by a sequence of triangular pulses

We now extend the analysis of section 4.3 to a sequence of triangular pulses. Obviously from figure 2(*d*) the pulse sequence that has the shape of a saw is characerized by three

parameters: the sweep rate v, the action duration T_1 and the out-of-action duration T_2. Mathematically, this pulse sequence depends on time as:

$$p(t) = \begin{cases} p_0 & \text{for } t \leqslant 0 \\ p_0 - v[t - (n-1)(T_1 + T_2)] & \text{for } (n-1)(T_1 + T_2) \leqslant t \leqslant (n-1) \\ & \quad \times (T_1 + T_2) + T_1 \\ p_0 & \text{for } n(T_1 + T_2) - T_2 \leqslant t \leqslant n(T_1 + T_2) \end{cases} \tag{4.37}$$

where $n = 1, 2, 3, \ldots$. Once more the action of such a time-dependent control input (4.37) together with the initial condition (4.15) leads to dynamical equations that can be solved exactly. Their solutions can be expressed as in (4.34) but with different $z_{2n-1}(t)$. After making the appropriate change of variables

$$t \to \mu_n = \{p_0 - v[t - (n-1)(T_1 + T_2)]\}v^{-2/3} \tag{4.38}$$

we derive the following formula for z_{2n-1}:

$$z_{2n-1}(t) = v^{1/3}\frac{\mathrm{Ai}'(\mu_n) + \nu_n \mathrm{Bi}'(\mu_n)}{\mathrm{Ai}(\mu_n) + \nu_n \mathrm{Bi}(\mu_n)} \tag{4.39}$$

which is formally similar to (4.28) but with a different definition of ν_n,

$$\nu_n = -\frac{v^{1/3}\mathrm{Ai}'(\varphi) - z_{2n-2}[(n-1)(T_1 + T_2)]\mathrm{Ai}(\varphi)}{v^{1/3}\mathrm{Bi}'(\varphi) - z_{2n-2}[(n-1)(T_1 + T_2)]\mathrm{Bi}(\varphi)} \tag{4.40}$$

where $\varphi = p_0\, v^{-2/3}$ and $z_0 \equiv z(0)$. With similar physics as in the previous case we can expect that the switching will be more favourable for longer action duration T_1 and/or shorter out-of-action duration T_2. This is confirmed graphically from figures 7(*a*), (*b*) and (*c*), which are plotted in the zp plane for the same $v = 0.01$ but different T_1 and T_2.

5. Conclusion

In conclusion, we have performed a local treatment of the switching process in excitonic optical bistability in semiconductors under the action of several kinds of time-dependent control inputs. The only asymptotic assumption is that of fully developed bistability, which makes it possible to expand the physical variables near the limit points in power series of a small parameter ϵ. This parameter is inversely proportional to the difference between the input field frequency and the excitonic frequency scaled to the exciton transverse damping. In typical semiconductors, the exciton transverse damping is about 1 meV while its binding energy ranges from some tens to some hundreds of meV (for instance, it is 33 meV for CdS and 200 meV for CuCl). Then one can choose the exciton detuning of 10 to 100 meV to observe OB. Such situations satisfy our asymptotic assumption on the smallness of ϵ. All the results have been obtained in terms of closed analytical expressions that allow one to understand easily the dynamics of the switching. The macroscopic nonlinear differential equations (2.10)–(2.13) have been derived from first principles based on a microscopic model taking into account the elementary interactions between photons, excitons and the driving field. A numerical simulation of the evolution equations (to be reported in a separate publication) has also shown that these differential equations can display complex dynamics including periodic and chaotic solutions. We therefore hope that such spontaneously pulsating solutions as well as their corresponding bifurcation diagrams could also be described analytically using a local approach. Such work is currently in preparation.

Acknowledgments

This research was supported in part by the Fonds National de la Recherche Scientifique and the Inter-University Attraction Pole programme of the Belgian government.

References

[1] Gibbs H M, McCall S L, Venkatesan T N C, Gossard A C, Passner A and Wiegmann W 1979 *Appl. Phys. Lett.* **35** 451
[2] Miller D A B, Smith S D and Johnston A 1979 *Appl. Phys. Lett.* **35** 658
[3] Bowden C M and Sung C C 1984 *Phys. Rev.* A **29** 1957
[4] Sung C C and Bowden C M 1985 *Phys. Rev.* A **31** 1936
[5] Koch S W, Schmidt H E and Haug H 1985 *J. Lumin.* **30** 232
[6] Rossmann H and Henneberger F 1984 *Phys. Status Solidi* b **121** 685; 1985 *Phys. Status Solidi* b **131** 185
[7] Mandel P and Erneux T 1982 *Opt. Commun.* **42** 362
[8] Bonifacio R and Lugiato L A 1976 *Opt. Commun.* **19** 172; 1978 *Phys. Rev.* A **18** 1129
[9] Mandel P 1986 *Frontiers in Quantum Optics* ed E R Pike and S Sarkar (Bristol: Adam Hilger) p 430; 1988 *Optical Bistability, Instability and Optical Computing* ed H Y Zhang and K K Lee (Singapore: World Scientific) p 118
[10] Moskalenko S A, Rotaru A H and Zaloj V A 1988 *Phys. Status Solidi* b **150** 401
[11] Khadzi P I and Shibarshina G D 1987 *Fiz. Tverd. Tela* **21** 1796
[12] Nguyen Ba An 1990 *Acta Phys. Pol.* A **78** 627
[13] Haug H and Koch S W 1990 *Quantum Theory of the Optical and Electronic Properties of Semiconductors* (Singapore: World Scientific)
[14] Kaplan I G and Ruvinskii M A 1976 *Zh. Eksp. Teor. Fiz.* **71** 2142
[15] Nguyen Ba An and Hoang Ngoc Cam 1990 *J. Phys.: Condens. Matter* **2** 4127
[16] Hanamura E 1970 *J. Phys. Soc. Japan* **29** 50; 1974 *J. Phys. Soc. Japan* **37** 1545
[17] Nguyen Ba An 1988 *Phys. Status Solidi* b **150** 845; 1989 *J. Phys.: Condens. Matter* **1** 843
[18] Nguyen Ba An, Hoang Ngoc Cam and Nguyen Trung Dan 1991 *J. Phys.: Condens. Matter* **3** 3317
[19] Glauber R 1963 *Phys. Rev.* **131** 2766
[20] Lindberg M, Koch S W and Haug H 1986 *J. Opt. Soc. Am.* **33** 751
[21] Nguyen Ba An and Le Thi Cat Tuong 1990 *Solid State Commun.* **76** 1139
[22] Mandel P 1988 *Instabilities and Chaos in Quantum Optics II* ed N B Abraham, F T Arecchi and L A Lugiato (New York: Plenum) p 321
[23] Segard B, Zemmouri J and Macke B 1987 *Opt. Commun.* **63** 339
[24] Mitschke F, Boden C, Lange W and Mandel P 1989 *Opt. Commun.* **71** 385
[25] Mandel P 1985 *Opt. Commun.* **55** 293
[26] Abramowitz M and Stegun I A 1972 *Handbook of Mathematical Functions* (New York: Dover)
[27] Boden C, Mitschke F and Mandel P 1990 *Opt. Commun.* **76** 178